

# Characterization of the Martian Surface Layer

GERMÁN MARTÍNEZ \*

UNIVERSIDAD COMPLUTENSE DE MADRID, MADRID, SPAIN

FRANCISCO VALERO

UNIVERSIDAD COMPLUTENSE DE MADRID, MADRID, SPAIN

LUIS VÁZQUEZ

UNIVERSIDAD COMPLUTENSE DE MADRID, MADRID, SPAIN

*Journal of Atmospheric Sciences*, Vol **66**, Issue 1, 187-198. DOI: 10.1175/2008JAS2765.1

## Abstract

We have estimated the diurnal evolution of Monin-Obukhov length, friction velocity, temperature scale, surface heat flux, eddy-transfer coefficients for momentum and heat, and turbulent viscous dissipation rate on the Martian surface layer for a complete Sol belonging to the Pathfinder mission. All these magnitudes have been derived from in situ wind and temperature measurements at around 1.3 m height, and simulated ground temperature (from 6 a.m. Sol 25 to 6 a.m. Sol 26). Up to the moment, neither values of turbulent viscous dissipation rate and eddy-transfer coefficients from in situ measurements for the Martian surface layer, nor diurnal evolutions of all the previous mentioned turbulent parameters for the Pathfinder had been obtained.

Monin-Obukhov similarity theory for stratified surface layers has been applied to obtain the results. The values assigned to the surface roughness, and the applied parameterization of the interfacial sublayer will be discussed in detail due to the sensibility of the results on them.

We have found similarities concerning the order of magnitude and qualitative behaviour of Monin-Obukhov length, friction velocity and turbulent vis-

cus dissipation rate on Earth and on Mars. However, magnitudes directly related to the lower Martian atmospheric density and thermal inertia, like temperature scale and hence surface heat flux, show different order of magnitude. Finally, turbulent exchanges in the first meters have been found to be just two orders of magnitude higher than the molecular ones, while on Earth around five orders of magnitude separate both mechanisms.

## 1 Introduction

The Planetary Boundary Layer (PBL) can be defined as that part of the atmosphere that is directly influenced by the presence of the planet surface, and responds to surface forcings with a timescale of about an hour or less. Belonging to the PBL, the Surface Layer is the region at the bottom of the PBL where turbulent fluxes and stress vary by less than 10% of their magnitude [23]. The sharpest variations in meteorological magnitudes take place in this layer, and, consequently, the most significant exchanges of momentum, heat, and mass [2].

The study of the Martian Surface Layer (MSL) becomes essential for two reasons. The first one concerns practical issues. Topics like variation rates of a magnitude associated with a concrete process (sampling rate required to capture a phenomenon) are needed for the design of the sensors. The second reason lies in the feedback between different scale processes. Phenomena with different time scales are interrelated as it happens on Earth. That is, the dynamic of the MSL affects mesoscale and synoptic phenomena, whose characterizing time scales

---

\* *Corresponding author address:* Germán Martínez, Dept. de Matemática Aplicada, Facultad de Informática, Universidad Complutense de Madrid, Av. Complutense s/n, Madrid, MA 28040, Spain.  
E-mail: mmgerman@fis.ucm.es

are larger. And the reverse is also true. Consequently, understanding all time scale phenomena is necessary to a better understanding of each of them.

The research of the MSL entails great drawbacks associated to the lack of suitable data. Only Viking and Pathfinder (PF) missions have provided in situ suitable meteorological data (high resolution temperature vertical profiles have been monitored by Mars Exploration Rover, although these data are not yet available). Viking landers [8] measured pressure, wind, and temperature at one height with a maximum sampling rate of about 0.8 Hz, used during periods spanning around one hour. On the other hand, PF lander [21] measured pressure at one height and temperature at three different heights, with a nominal sampling rate of 0.25 Hz, and a maximum sampling rate of 1 Hz for periods not longer than 1h. Unfortunately, the wind sensor experienced problems and wind data are not available in the Planetary Data Science.

Seminal works have been done from these sparse in situ data. [24] showed the diurnal behaviour of Monin-Obukhov length, friction velocity and surface heat flux for the first 45 Sols (1 Sol corresponds to one Martian day, approximately 24.7 h) based on wind and temperature data measured by the Viking landers. Some years after, [17] developed a one dimensional boundary layer model which simulated the diurnal behaviour of the surface heat flux for the Viking mission, and was also used to compare in situ Viking data (wind, temperature, and vertical profiles during the entry) to the outputs of the model. Another one dimensional boundary layer model, in which the diurnal evolution of surface heat flux and friction velocity for the first Sols of Viking mission were simulated, was developed by [6]. Wind and temperature spectra from in situ wind and temperature measurements were carried out by [25] for the Viking mission. In that paper, Monin-Obukhov length diurnal evolution for one day was shown as well as values for specific hours of friction velocity and surface heat flux. [18] and [14] estimated values of Obukhov length and eddy-diffusion coefficients, and simulated the diurnal evolution of surface heat flux for the PF mission based on Sävijärvi one dimensional boundary layer model [17]. [12] carried out a similar research to the one employed by [25], and studied the wind and temperature spectra for the PF mission from in

situ wind and temperature measurements for specific hours, although neither diurnal evolutions nor single values of Monin-Obukhov length, friction velocity and temperature scale were given.

[24], [25], and [12], who used in situ wind and temperature data, needed the help of Monin-Obukhov similarity theory to yield diurnal evolutions of turbulent parameters. The reason relies on two facts. Firstly, wind vertical component has never been measured on Mars. And even if it had been measured, turbulent parameters like friction velocity and temperature scale would have not been accurately obtained by the covariance method due to the low sampling rate used. As a consequence, turbulent magnitudes on Mars can only be obtained from mean variables (by mean variables we refer to 1h averaged values). And this is exactly the *modus operandi* of Monin Obukhov similarity theory and the reason why this theory is widely used in the research of the MSL.

It can be noticed that no diurnal evolution of turbulent parameters from in situ data has been reported in the above mentioned literature for the PF mission. The main reason is due to the problem experienced by the wind sensor, for which wind data are not available in the Planetary Data Science. However, we have been recently given by Dr Jim Murphy quality controlled wind data for a complete Sol with a sampling rate of 0.25 Hz, covering from 6 a.m. Sol 25 to 6 a.m. Sol 26 [in situ PF wind data corresponding to other Sols, in which measurements did not cover the whole day continuously, have been used by other authors: [12], [14], and [19].

These in situ wind data, in situ temperature measured at the top height of the lander mast, and hourly simulated ground temperature obtained from the one-dimensional boundary layer model [19] form the inputs of this work. From them, the diurnal evolution of the main turbulent parameters for the PF landing area has been obtained. Monin Obukhov length, friction velocity, temperature scale and consequently surface heat flux, whose diurnal evolutions had already been obtained for the Viking mission from in situ measurements, will be shown for the PF in this paper. Finally, we have derived the daily behaviour of turbulent viscous dissipation rate and eddy diffusion coefficients whose values had not yet been given before from in situ measurements for the MSL.

The inputs, specially wind data, will be discussed in section 2. Section 3 is divided into two parts. We shall study the applicability of the Monin-Obukhov similarity theory for stratified surface layers on Mars first, and then the method employed to derive the results will be detailed. Issues related to the value of the surface roughness and the parameterization of the interfacial sublayer will be emphasized. In section 4, we will show diurnal evolutions of all the parameters under study for the different proposed values of the surface roughness. Moreover, those parameters which are sensitively affected by the inclusion of the interfacial sublayer will be shown separately to explain how they change. Section 4 will be closed by making a comparison between the herein obtained Martian results and the known terrestrial counterparts in order to highlight the main differences between both planets. Finally, we will summarize the main conclusions in section 5.

## 2 Data

Three set of data form the inputs of this paper: in situ observed wind and temperature measurements, and simulated ground temperature, all of them covering from 6 a.m. Sol 25 to 6 a.m. Sol 26 of PF mission (this period under study will be hereafter named named PS). Before explaining separately the characteristics of each of them, a brief summary of the PF mission will be given.

The PF lander touched down on July 4, 1997, at 19.7 N, 33.55 W in the Ares Vallis region of Chryse Planitia. It was northern summer at this time, corresponding to a solar longitude about 140 deg. The total duration of the mission was 83 Sols, although Sols 17, 31, 43, 45, 46, 48, and 51 contained no meteorology data. Through the other 76 Sols, pressure at one and temperature at three different heights were properly collected by the Meteorology Package Instrument while the wind portion of the system design was flawed. Continuous sampling for a complete Sol at 0.25 Hz was conducted on Sols 25, 32, 38, 55, and 68 while the nominal strategy consisted of measuring 51 equally spaced times for 3 min during the first 30 Sols. During the extended mission (Sols 31-83) the Meteorology Package Instrument data were monitored inside the hours 0900-1500 local solar time (LST).

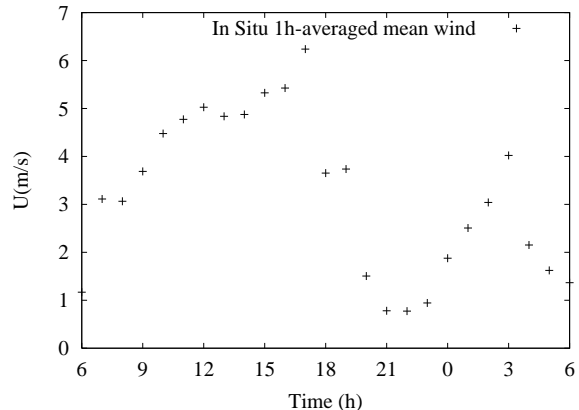


Figure 1: Diurnal evolution of the 1h-averaged wind speed for Sols 25-26 from Pathfinder lander.

A review of the reliability of the inputs is now given, since the accuracy of the results depends on the former. We start with wind data. PF wind sensor experienced problems related to the overheat temperature of the sensor wire segments from which wind speed was derived. The lack of a representative temperature that could serve as a baseline against which overheat could be determined caused the failure. Thermocouple gas-temperature measurements has been used as an alternative to provide a valid representation of unheated wire temperatures.

By this way, wind data monitored with a sampling rate of 0.25 Hz covering the PS have been provided. The main uncertainties of the derived wind data concentrate over the daytime due to the short time large temperature fluctuation, whereas from around 5 p.m. to 6 a.m., when strong stability makes temperature fluctuations small, wind speeds present more confidence. Fig. 1 shows the 1h-averaged wind data (at a height of 1.09 m above the lander petals, that is, around 1.30 m above the ground). As the local instability increases convection gets stronger, mixing the air at 1.3 m with air from above where wind velocity is higher. The result is the peak observed around 4 p.m., see Fig. 1. This behaviour and the magnitude of the wind match with those found in Viking mission and with those occurring on Earth.

The second observed maximum is supposed to be related to the frictional decoupling caused by the

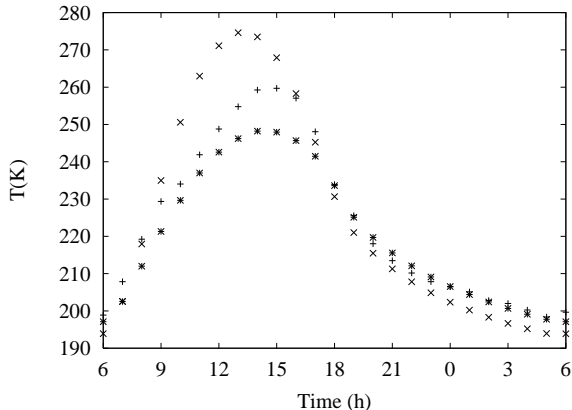


Figure 2: The figure shows three diurnal evolutions of temperature for Sols 25-26: i) 1h-averaged in situ temperature at 1.27 m (+). ii) Simulated temperature at the same height (\*). iii) Simulated ground temperature (x).

mixed layer collapse after sunset. The formed martian nocturnal low-level jet [20] would create a high turbulent kinetic energy layer which, through shear mechanism (expected to be very important due to the strong night-time inversions), could propagate downwards. The result would be this local maximum, which can also be observed in [19].

We now turn to temperature measurements. Temperature was monitored at three different heights on the mast of the PF lander. The top height measured 1.27-m temperature has been used in this work for two reasons. It is supposed to be the less contaminated by the thermal radiation of the lander, and the height virtually matches the wind sensor height (about 1.30 m), which is required for the employed methodology. The sampling rate used was 0.25 Hz during the PS, as for wind. We represent the 1h-averaged temperature in Fig. 2. The diurnal temperature behaviour is quite typical as the Sol-to-Sol temperatures have been very repeatable over the first 30 Sols [12]. Maximum temperature, about 260K, is reached between 14-15 LST. The minimum, around 195K, is observed by 5 a.m., just before sunrise.

To close the characterization of the inputs, simulated ground temperature is discussed. A one-dimensional boundary layer model [19], kindly

shared by Prof. Sävijärvi, has been used to estimate hourly outputs of ground temperature during the PS. In this paper, this model has been slightly modified, and values of 0.19 and  $387 \text{ J m}^{-2} \text{ K}^{-1} \text{ s}^{-1/2}$  for albedo and thermal inertia, respectively, have been used to run the model, and to create the most probably scenario for the ground temperature, see Fig. 2. In addition, two other extreme scenarios, the warmest and the coldest, have been created by using extreme reliable values of surface emissivity [4], dust optical depth [11], and finally albedo and thermal inertia [16] for the PF location. In situ temperature measurements at the bottom height has also been considered for creating such scenarios. It has been used as a lower limit for the ground temperature during the daytime, while at night, as an upper limit instead. As a result, ground temperature has been reduced 4 K and 3 K during the night-time and daytime respectively in the coldest scenario, while concerning the warmest, 8 K have been added during the daytime and around 2 K at night. The sensitivity of the results to these limiting cases will be commented later.

It is worth to mention that even though only one day has been used, it is highly expected to represent a well-typical day of the northern summer for the PF landing region. The reason was the small influence of the atmospheric distortion and variability that took place for the first 30 Sols.

Summarizing, 900 observed wind and temperature data, corresponding to  $\pm 30$  min (0.25 Hz sampling rate) from each specific hour, have been averaged to yield hourly inputs from 6 a.m. Sol 25 to 6 a.m. Sol 26. By employing this time average, long term trends are filtered and only turbulence is expected to remain [23]. Thus, 25 hourly inputs both for temperature and wind, and 25 simulated ground temperatures hourly inputs have been used to compute the values of the turbulent parameters obtained.

### 3 Methodology

The previous data set as an input, K-theory, and Monin-Obukhov similarity theory for stratified surface layers will be used in order to estimate the diurnal behaviour of Monin-Obukhov length  $L$ , friction velocity  $u_*$ , temperature scale  $T_*$ , dynamic

surface heat flux  $H_0$ , turbulent viscous dissipation rate  $\epsilon$ , and eddy diffusivity coefficients for momentum  $k_m$  and heat  $k_h$ .

Before showing in detail the method employed to derive the results, a brief explanation of the applicability of the similarity theory for stratified surface layers on Mars will be given.

### 3.1 On the applicability of the similarity theory on Mars

In order to employ the similarity theory some hypothesis should be met. We shall enumerate these hypothesis and explain to what extent they agree on Mars.

Assuming a horizontally homogeneous and quasi-stationary surface layer where turbulent fluxes are not dependent on height, and that both Coriolis effect and molecular exchanges are neglected, magnitudes concerning the mean flow and turbulent characteristics do depend only on four independent variables: buoyancy parameter  $g/T_g$ , height above the ground  $z$ , surface drag or equivalently friction velocity  $u_* = \sqrt{|\tau_0|/\rho}$ , and kinematic surface heat flux  $H_0/\rho c_p$  [15]. As these four variables involve only three fundamental dimensions, Buckingham Pi Theorem states that only one dimensionless parameter can be formed,  $\zeta = z/L$ , where

$$L = -\frac{u_*^3}{k \frac{g}{T_g} \frac{H_0}{\rho c_p}}$$

is the Monin-Obukhov length. In addition, any other dependent variable, when made dimensionless by the fundamental scales  $z$ ,  $u_*$ , and  $T_* = -H_0/\rho c_p u_*$  (formed with three of the independent variables) is a unique function of  $\zeta = z/L$ .

We shall treat separately each of the required hypotheses to use the similarity theory on Mars. The complexity of the terrain along with large scale phenomena (synoptic perturbations) can greatly alter horizontal homogeneity. However, synoptic perturbations were not present at the time and location of the study, and the landing site, although not specially flat, did not present a sharp topography [5]. On the other hand, we have found in this work molecular exchanges to be two orders of magnitude lower than turbulent diffusion in the first meters, which still allow to neglect molecular diffusion in

the surface layer. Moreover, the height of the surface layer and the magnitude of the Coriolis force are found to be of the same order than on Earth and consequently Coriolis force can be neglected. Concerning the suspended dust, similarity theory does not take into account this Martian phenomenon (neither of the independent variables takes direct notice of dust). Nevertheless, the observed dustiness was low [18] and the importance of the dust became reduced. Finally, the analytical form in which any dimensionless variable depends on the dimensionless parameter  $\zeta = z/L$  (e.g., universal functions for momentum and heat) has been supposed to be the same as on Earth.

### 3.2 The Bulk method. Universal functions, roughness length and the interfacial sublayer

The method employed to obtain the results will be explained in this section. In addition, the values assigned to the surface roughness length  $z_0$ , the inclusion of the interfacial sublayer (that layer of air in which the transfer of momentum and heat is dominated by molecular processes), and the analytical form of the universal functions for heat and momentum will be carefully described.

Due to the nature of the inputs, the Bulk method [2] has been used. Mean wind and mean temperature measured at the same height (we will suppose the same height for wind and temperature measurements, since only about 3 cm separate them), as well as ground temperature are needed by this method. Following this approach, the bulk Richardson number can be written like

$$R_B = \frac{g}{T_g} \frac{(T - T_g)z}{U^2} \quad (1)$$

where  $g$  is the Martian surface gravity ( $=3.7 \text{ m s}^{-2}$ ),  $T_g$  is the surface temperature, and  $z$  is the height where wind,  $U$ , and temperature,  $T$ , have been monitored. Several hypotheses have been taken into account to derive the analytical form of (1): the mean wind has been supposed to be aligned with the x-axis, subsidence has been neglected, virtual potential temperature has been substituted by the standard temperature [25], and turbulent fluxes of momentum  $\overline{u'w'}$  and heat  $\overline{w'T'}$  have been parameterized with equal diffusion coef-

ficients ( $k_m = k_h$ ) via K-theory:

$$\overline{u'w'} = -k_m \frac{\partial U}{\partial z} \quad (2)$$

$$\overline{w'T'} = -k_h \frac{\partial T}{\partial z} \quad (3)$$

Substituting  $T - T_g$  and  $U^2$  into (1) from the integration of the similarity relationships

$$\frac{kz}{u_*} \frac{\partial U}{\partial z} = \phi_m(\zeta) \quad (4)$$

$$\frac{kz}{T_*} \frac{\partial T}{\partial z} = \phi_h(\zeta) \quad (5)$$

leads to

$$\frac{g}{T_g} \frac{(\bar{T} - T_g)z}{\bar{U}^2} = \zeta \frac{\int_{\zeta_{0T}}^{\zeta} \zeta'^{-1} \phi_h(\zeta') d\zeta'}{\left(\int_{\zeta_0}^{\zeta} \zeta'^{-1} \phi_m(\zeta') d\zeta'\right)^2} \quad (6)$$

with  $\zeta_0 = z_0/L$  and  $\zeta_{0T} = z_{0T}/L$ , where the surface roughness  $z_0$  is defined as that height in which wind speed vanishes according to (4), and  $z_{0T}$  corresponds to the surface skin temperature, i.e., the measurable radiative temperature. Notice that the assumption  $k_m = k_h$  is not needed. Solving (6), the dimensionless parameter  $\zeta = z/L$  is obtained for each hour and hence friction velocity, temperature scale, surface heat flux, eddy diffusion coefficients and viscous dissipation rate are derived too, as it will be seen below.

Before solving (6), two issues must be faced: the analytical form of the universal functions  $\phi_m$  and  $\phi_h$  appearing in (4) and (5), and the values assigned to  $z_0$  and  $z_{0T}$  in (6).

We have chosen the analytical form of the universal functions estimated by [10]:

$$\phi_m(z/L) = \begin{cases} (1 - 19.3z/L)^{-\frac{1}{4}}, & -2 < z/L < 0 \\ 1 + 6z/L, & 0 < z/L < 1 \end{cases} \quad (7)$$

$$\phi_h(z/L) = \begin{cases} 0.95(1 - 11.6z/L)^{-\frac{1}{2}}, & -2 < z/L < 0 \\ 0.95 + 7.8z/L, & 0 < z/L < 1 \end{cases} \quad (8)$$

Very similar results have obtained with the use of Businger (1971), and Dyer (1974) universal functions and therefore they are not shown.

Concerning the value given to  $z_0$ , [24] estimated values of  $z_0$  between 0.1 and 1 cm for the Viking

missions, while [6] indicated that a better upper limit could be 10 cm. For the PF mission, [12] derived the value of  $z_0$  from the images of the surroundings of the lander as reported in [22], and assigned a value of 1 cm after having applied Lettau's formula [13]. Nevertheless, based on the existing uncertainties, values of 0.1, 1 and 10 cm have been used in this work.

The last matter is related to the use of a molecular sublayer and consequently with the value given to  $z_{0T}$ . Noticing that  $\rho_{Mars}/\rho_{Earth} \sim 10^{-2}$  and the composition of the air, molecular kinematic viscosity and molecular thermal diffusivity [both on the order of  $10^{-3} \text{ m}^2 \text{ s}^{-1}$  on Mars, [24] are two orders of magnitude higher on Mars than on Earth. The molecular sublayer will definitely be more in evidence in Mars and its inclusion becomes more necessary since similarity theory neglects molecular processes. A parameterization for this sublayer corresponding to surfaces with bluff impermeable elements will be proposed.

## 4 Results

First of all, results without the inclusion of the molecular sublayer are shown, that is, assuming  $z_{0T} = z_0$ . Diurnal evolutions, dependences on the parameter  $z_0$ , and comparisons to other Martian papers are presented. Then, the inclusion of the molecular sublayer is done and the affected magnitudes described. Finally, a comparison between orders of magnitude on Earth and on Mars is carried out for all the obtained parameters.

### 4.1 Case Study I: No molecular sublayer

#### 4.1.1 Monin-Obukhov Length

Solving the implicit Eq.(6) for each of the different values of  $z_0$ , Monin-Obukhov length is obtained. By definition  $L$  is negative under local static instability conditions. As can be seen in Fig. 3, over much of the daytime when convection is very strong, its value becomes negative and close to zero (about -25 m for  $z_0 = 1\text{cm}$ ). At night, it becomes positive following the nocturnal local static stability. Around sunrise and sunset, the values of  $L$  seem to diverge. However, this behaviour has no

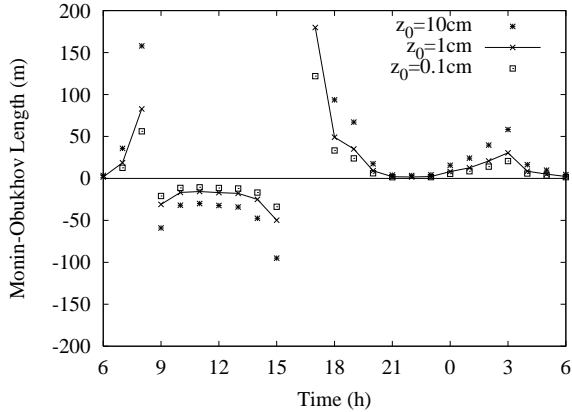


Figure 3: Diurnal evolution of the Monin-Obukhov length for the different proposed surface roughness values. Pathfinder mission, Sols 25-26.

physical meaning since the obtained surface heat flux vanishes momentarily as ground temperature equals temperature at the height of the sensor. Therefore, the applicability of the M-O similarity theory for thermally stratified surface layers is no longer valid given that the surface layer is not thermally stratified in the first meter at that moment. This magnitude has been found to vary less than 20% when it has been determined under the ground temperature extreme scenarios.

Another important aspect is that which refers to the increase in the value of  $L$  with  $z_0$  displayed in the same Fig. 3. Since its absolute value is thought to be proportional to the height of the layer where shear effects dominates on buoyancy effects, the higher the terrain roughness becomes the more important the shear effects are, and consequently  $L$ .

The hyperbolic diurnal behaviour and the order of magnitude match with those found by [24] and [25] in Viking Lander 2 for early summer and early spring respectively.

#### 4.1.2 Friction velocity and surface heat flux

Once the dimensionless parameter  $\zeta = z/L$  is obtained from (6), it is straightforward to derive the diurnal evolution for  $u_*$  integrating (4).

Friction velocity represents the turbulent vertical exchange of horizontal momentum between the

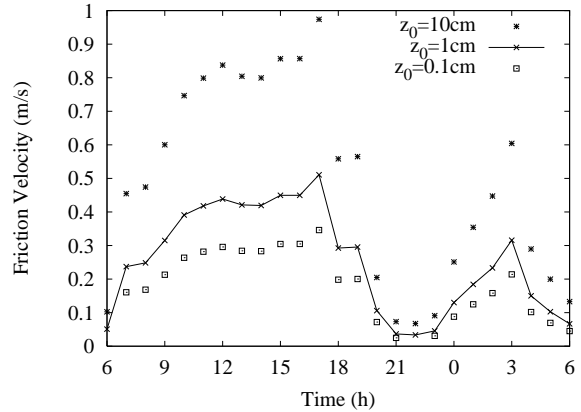


Figure 4: Diurnal evolution of friction velocity for the different proposed  $z_0$  values. Pathfinder mission, Sols 25-26.

ground and the first meters of the atmosphere. Thus, it is reasonable to expect maximum values when the 1.3 m-wind peaks since the shear becomes maximum. This behaviour is observed in Fig. 4, where  $u_*$  follows the evolution of the mean wind (see Fig. 1), although modulated by the prevailing stability. It can also be noticed that friction velocity grows with the parameter  $z_0$  since more horizontal momentum is lost to the ground if the surface becomes more roughness. Its magnitude is of the order of  $0.1 \text{ m s}^{-1}$  for the proposed values of  $z_0$ , and its values vary less than 5% when the extreme scenarios for the ground temperature are imposed. Similar quantitative results have been obtained by [24], [25], and [6] for Viking Lander 1 and 2 in the early summer. However, the second peak is not so evident in these works.

Temperature scale  $T_*$  has been obtained by integrating (5). This parameter represents the typical eddy temperature fluctuations in the surface layer. In this work, values of  $T_*$  of the order of 1 K for the convective daytime have been obtained. This magnitude is consistent with the temperature fluctuations observed by the PF lander since in minutes, changes of the order of magnitude of 1 K could be appreciated. As an alternative way,  $T_*^{alt}$  has also been calculated using the above derived  $z/L$  values, and the in situ temperature measurements at 0.52, 0.77 and 1.3 m. Assuming neutral stability conditions,  $T_*^N = kz\partial T/\partial z$  has been calculated

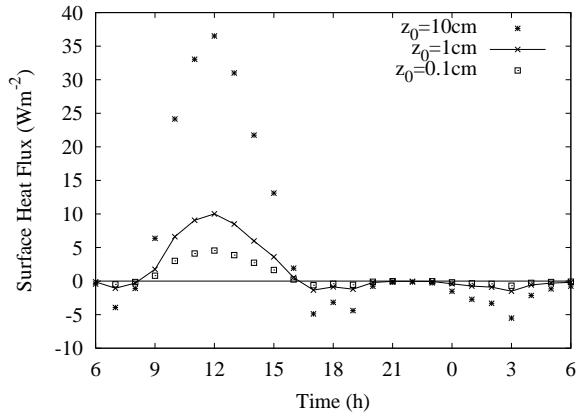


Figure 5: Diurnal evolution of the dynamic surface heat flux for the different proposed  $z_0$  values. Pathfinder mission, Sols 25-26.

from these three heights. Taking advantage of the obtained  $\phi_h(z/L)$  values (see (8) with  $z/L$  calculated via (6)), it is a good approximation to state  $T_*^{alt} = T_*^N / \phi_h(z/L)$ , see (5). The matching between the scale temperature values determined by this approach and the ones previously obtained is quite good. In both cases, the order of magnitude under stability conditions is of 0.1 K, while under unstability is of 1 K (maximum values around 5 K).

Instead of representing its diurnal evolution, we have shown the dynamic surface heat flux

$$H_0 = -\rho c_p u_* T_* \quad (9)$$

in Fig. 5. It is positive (directed upwards) during the daytime when local static instability conditions prevail as ground is warmer than the first few meters of the atmosphere, and negative during the night, when the first meters become statically stable. The flux is maximum at noon,  $\sim 10 \text{ W m}^{-2}$  for  $z_0=1 \text{ cm}$ , because though friction velocity reaches its maximum later (Fig. 4), the difference between ground and sensor temperature (Fig. 2) causes  $T_*$  to peak at this time. The rest of the day it remains close to zero due to the attenuation of turbulence ( $u_*$  diminishes) and the decreasing of the difference between air and ground temperature. As in the case of Monin-Obukhov length, surface heat flux varies less than 20% in the extreme scenarios.

Dynamic surface heat flux increases with the surface roughness as  $u_*$  and  $T_*$  do. Similar results have

been yielded by other authors for Viking mission, with maxima about  $\sim 10 \text{ W m}^{-2}$ . Concerning PF mission, [18] estimated maxima of  $14 \text{ W m}^{-2}$ .

#### 4.1.3 Turbulent viscous dissipation rate and eddy diffusivity coefficients

Based on the similarity theory, any magnitude involving no more fundamental dimension than time, longitude and temperature is a unique function of the parameter  $\zeta = z/L$  when made dimensionless by the fundamental scales  $z$ ,  $u_*$ , and  $T_*$ . As we know the values of these scales as well as the value of  $\zeta = z/L$ , eddy diffusivity coefficients for heat and momentum and turbulent viscous dissipation rate will be derived.

Starting with the diffusivity coefficients  $k_h$  and  $k_m$ , and noticing that their dimension are  $\text{m}^2 \text{ s}^{-1}$ , the term that makes the diffusivity coefficients dimensionless must be  $1/\kappa z u_*$ . Hence

$$k_m / \kappa z u_* = F(\zeta)$$

and

$$k_h / \kappa z u_* = G(\zeta)$$

where  $\kappa$  is the Von Karman constant, and  $F$  and  $G$  are unknown functions of the parameter  $\zeta$ . Taking into account that

$$\overline{u'w'} = -u_*^2 = -k_m \frac{\partial U}{\partial z} = -k_m \frac{u_*}{kz} \phi_m(\zeta)$$

and

$$\overline{T'w'} = -u_* T_* = -k_h \frac{\partial T}{\partial z} = -k_h \frac{T_*}{kz} \phi_h(\zeta)$$

where (2), (3), (4), and (5) have been used, the following relation is yielded for  $F$  and  $G$ :

$$F(\zeta) = \phi_m^{-1}(\zeta)$$

$$G(\zeta) = \phi_h^{-1}(\zeta)$$

with  $\phi_m$  and  $\phi_h$  given by (7) and (8). Eventually, the next relationships are derived for the eddy diffusivity coefficients:

$$\frac{kz u_*}{k_m} = \phi_m \quad (10)$$

$$\frac{kz u_*}{k_h} = \phi_h \quad (11)$$

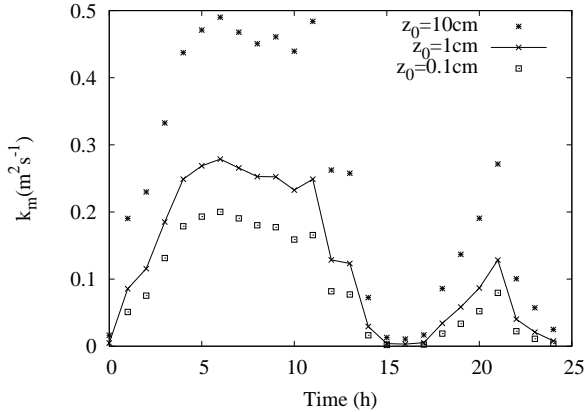


Figure 6: Diurnal evolution of the 1.3 m eddy diffusion coefficient for momentum for the different proposed  $z_0$  values. Pathfinder mission, Sols 25-26.

These parameters measure how efficient the atmosphere is in transporting momentum and heat via turbulent vertical fluxes. It is expected that the higher turbulent fluxes are the higher value this parameter takes. This behaviour, at 1.3 m height, is displayed in Figs. 6 and 7, where these coefficients tend to follow the friction velocity (Fig. 4). By construction,  $k_h$  is slightly higher than  $k_m$  in accordance with the universal functions employed and their values are of the order of  $0.1 \text{ m}^2 \text{ s}^{-1}$  (less than 5% of variation found in the extreme scenarios). Thus, turbulent diffusion is two orders of magnitude more efficient than molecular diffusion, since both molecular kinematic viscosity and molecular thermal diffusivity are of the order of  $10^{-3} \text{ m}^2 \text{ s}^{-1}$ .

We have also estimated values of  $k_m$  and  $k_h$  using the one-dimensional boundary layer model [19], and found that simulated values are slightly higher at 1.3 m, although the order of magnitude is the same.

Turbulent viscous dissipation rate has been derived similarly. Its dimensions are  $\text{m}^2 \text{ s}^{-3}$ , which implies that the dimensionless term that depends on  $\zeta$  has to be

$$\frac{kz\epsilon}{u_*^3} = f(\zeta) \quad (12)$$

The analytical relationship between these two dimensionless parameters can not be directly obtained as in the case of the diffusivity coefficients.

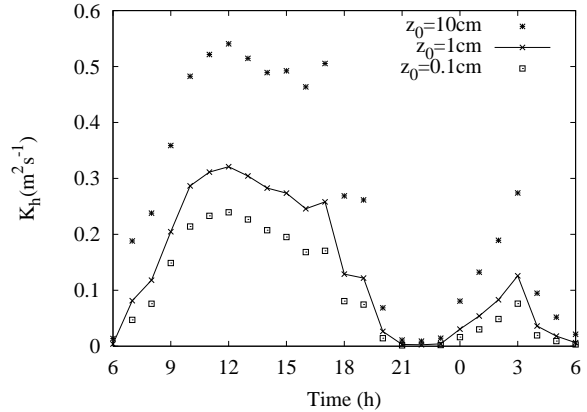


Figure 7: Diurnal evolution of the 1.3 m eddy diffusion coefficient for heat for the different proposed  $z_0$  values. Pathfinder mission, Sols 25-26.

However, [27] yielded an empirical relation :

$$\frac{kz\epsilon}{u_*^3} = \begin{cases} (1 + 0.5(z/L)^{2/3})^{3/2}, & z/L > 0 \\ [1 + 2.5(z/L)^{3/5}]^{3/2}, & z/L < 0 \end{cases} \quad (13)$$

Making use of this relationship, values of  $\epsilon$  are estimated. Turbulent viscous dissipation rate represent the conversion of turbulent kinetic energy into heat. As can be seen in Fig. 8, turbulent viscous dissipation rate peaks at the same time as the friction velocity and behaves similarly. This is because  $f(\zeta)$ , in which buoyancy effects are considered via  $L$ , does not significantly change the shape of  $u_*$ . The physical cause lies in that shear and dissipation are usually the dominant terms under stability conditions. Alternatively, under instability, buoyancy and turbulent transport, which are also important, tend to balance each other [27]. In both cases dissipation is virtually in accordance with the shear, presenting maximum values around  $0.1 \text{ m}^2 \text{ s}^{-3}$  during the daytime for  $z_0 = 1 \text{ cm}$ , while at night it becomes close to zero. The variation of this magnitude under the ground temperature extreme scenarios is lower than 5%. It is fair to say that the validity of (13) on Mars present uncertainties. Until specific experiments be conducted to measure the importance of each of the terms (shear, buoyancy, transport and dissipation) of the turbulent kinetic energy, it will not be possible to assure that the balances previously mentioned are met. Nevertheless,

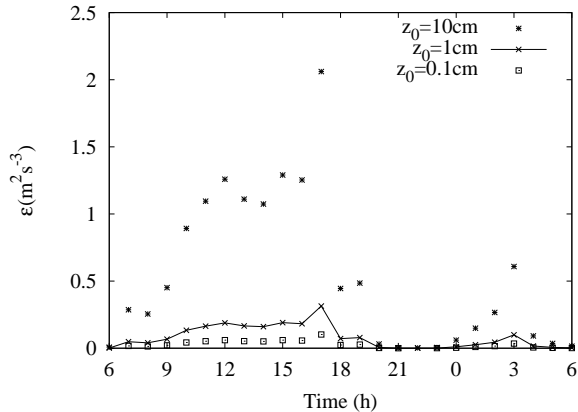


Figure 8: Diurnal evolution of the 1.3 m viscous dissipation rate for the different proposed  $z_0$  values. Pathfinder mission, Sols 25-26.

it is expectable that they will be met.

## 4.2 Case Study II: Inclusion of a molecular sublayer

The necessity of including the molecular sublayer into the similarity theory will be discussed. Those parameters which turned out to be affected by its inclusion will be shown, explaining how and why they have changed.

### 4.2.1 Need for molecular sublayer

Molecular kinematic viscosity and molecular thermal diffusivity are of the order of  $10^{-3} \text{ m}^2 \text{ s}^{-1}$  on Mars. Taking into account that we have found eddy-transfer coefficients to be of the order of  $10^{-1} \text{ m}^2 \text{ s}^{-1}$ , only two orders of magnitude separate both mechanisms on Mars. As similarity theory neglects molecular diffusion, we have followed the approach used by [29] and incorporated the molecular sublayer into the surface layer similarity theory by assuming a relation for  $z_0/z_{0T}$ . The difference between these two parameters tends to be greater for flow over bluff roughness elements [9], which makes even more important its inclusion on Mars.

The parameterization developed by [3] will be used. With aid of dimensional analysis and experiments, Brutsaert estimated the next relation for

surfaces with bluff impermeable elements:

$$\ln\left(\frac{z_0}{z_{0T}}\right) = 7.3kRe_0^{0.25}Pr^{0.5} - 5k \quad (14)$$

with  $k$  the von Karman constant,  $Re_0 = z_0u_*/\nu$  the roughness Reynolds number (where  $\nu$  represents the kinematic viscosity), and  $Pr$  the Prandtl number. Different parameterizations can be found in the literature for other type of soils, although this one is expected to represent more accurately the Martian soil.

### 4.2.2 Results

We have found that magnitudes directly related to  $z_{0T}$ , that is, temperature scale through

$$T_* = \frac{k(T(z) - Tg)}{\int_{\zeta_{0T}}^{\zeta} \zeta'^{-1} \phi_h(\zeta') d\zeta'} \quad (15)$$

and dynamic surface heat flux through (9), are sensitively affected by the inclusion of the molecular sublayer. Nevertheless, friction velocity and hence both turbulent viscous dissipation rate and eddy-transfer diffusivity coefficients are not. This behaviour is reasonable because in this sublayer only molecular transfer is important for heat, while for momentum, in addition to the molecular transport, pressure fluctuations are very relevant so the net effect on the transport of momentum is less noticeable [28].

The main consequences found with the inclusion of the molecular sublayer are: (i) a decrease of heat flux values for a given difference between air temperature and surface skin temperature, and (ii) a reduction of  $z_0$  dependence ( $z_{0T}$  lies in the range  $10^{-3} - 10^{-4} \text{ m}$  for all  $z_0$  values). Both aspects can be observed in Fig. 9 when it is compared to the values obtained without the inclusion of the molecular sublayer (see Fig. 5).

Similar results have been obtained for VL missions by [24] and [6] when a molecular sublayer was used. In both cases, the principal effect of adding a molecular sublayer was to reduce the influence of  $z_0$  on the heat fluxes, although for low values of  $z_0$  the surface heat flux in [24] did not decrease, while it did for larger values of  $z_0$ . [25] assumed the same  $z_{0T}$  for all values, after having parameterized  $z_{0T}$  in a similar way than we have had.

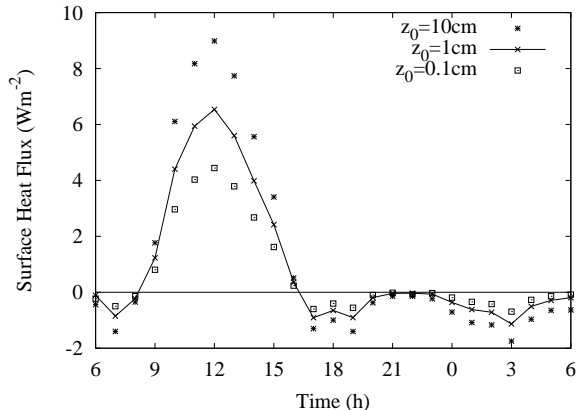


Figure 9: Surface Heat flux estimated with the inclusion of the molecular sublayer. Pathfinder mission, Sols 25-26.

### 4.3 Earth turbulent scales vs Martian turbulent scales

In this section we shall compare the order of magnitude of the herein obtained Martian parameters to those typically found on Earth, highlighting the main differences between both planets.

We start with the Monin-Obukhov length. Values of  $L$  have been found to range between 0 and 100 m. These values also correspond to those typically found on Earth. That is, the height of the surface layer fits on both planets. On the other hand, we have derived values around  $0.1 \text{ m s}^{-1}$  for the friction velocity, that turn out to be of similar magnitude as on Earth [1].

Concerning the surface dynamic heat flux, maximum values around  $10 \text{ W m}^{-2}$  have been obtained. In desert environments, like Gobi desert [7], maximum values are one order of magnitude higher instead. This is due to the lower Martian atmospheric density, given that  $\rho_{Mars}/\rho_{Earth} \sim 10^{-2}$  and that the specific heat capacities  $c_p$  are of the same order on both planets (around  $730 \text{ J K}^{-1} \text{ Kg}^{-1}$  on Mars and  $1004 \text{ J K}^{-1} \text{ Kg}^{-1}$  on Earth). According to the definition of  $H_0$  in (9), and noticing that friction velocities have the same magnitude on both planets, we conclude that maximum values of the temperature scale  $T_*$  can reach one order of magnitude higher on Mars (remember that maximum  $H_0$  values are one order of magnitude higher on Earth and

that the term  $\rho c_p$  is two orders of magnitude higher on Earth). Actually, values around 5 K has been found for  $T_*$  in this paper, while values between 0.1 and 1 K are typical for Earth. The difference can be explained as follow: surface energy budget is almost driven by radiation and virtually balanced by heat conduction in the soil (latent and sensible fluxes are much smaller in magnitude). In addition, Martian ground present low values of thermal inertia. Both aspects cause Martian ground to warm and cool up to around 80 K daily. Since air from above can not follow the soil temperature evolution so rapidly (low atmospheric density), large temperature gradients are created, resulting in higher temperature scales.

Finally, the efficiency of both molecular and turbulent diffusion will be treated. Gathering the values of molecular and turbulent diffusion coefficients for both heat and momentum on both planets, Table 1 is formed, where terrestrial values of  $k_m$  and

Table 1: Values for the molecular and turbulent diffusion coefficients on Mars and on Earth.  $k_m$  and  $k_h$  represent turbulent diffusion coefficients for momentum and heat respectively at around 1.3 m. Kinematic molecular viscosity is represented by  $\nu$  and thermal molecular diffusivity by  $\kappa$

	$\nu(m^2 s^{-1})$	$\kappa(m^2 s^{-1})$	$k_m(m^2 s^{-1})$	$k_h(m^2 s^{-1})$
Mars	$\sim 10^{-3}$	$\sim 10^{-3}$	$\sim 10^{-1}$	$\sim 10^{-1}$
Earth	$\sim 1.5 \times 10^{-5}$	$\sim 2 \times 10^{-5}$	$\sim 1 - 10^1$	$\sim 1 - 10^1$

$k_h$  has been taken from [23], and values of the Martian eddy-diffusion coefficients at 1.3 m from this study. It can be seen that turbulent diffusion is five or six orders of magnitude more effective than molecular diffusion on Earth. However, this behaviour is different on Mars as turbulent diffusion is only two orders of magnitude more effective than molecular diffusion.

## 5 Discussion and Conclusions

Diurnal evolutions of Monin-Obukhov length, friction velocity, dynamic surface heat flux, eddy-transfer coefficients, and turbulent viscous dissipation rate have been determined for one complete

PF Martian Sol. Neither diurnal evolutions of the mentioned parameters, nor values of turbulent viscous dissipation rate and eddy-transfer coefficients had been given from in situ wind and temperature measurements for the PF.

The reason might lie in the problem experienced by the wind sensor located on the PF lander. Due to the overheat temperature of the sensor wire segments, from which wind speed had to be derived, in situ wind data are not available in the Planetary Data Science. However, thermocouples gas-temperature has been expected to provide a valid representation of unheated wire temperature. By employing them, Dr Murphy (New Mexico University) has kindly given us wind data covering from 6 a.m. Sol 25 to 6 a.m. Sol 26. In situ top height measured temperature over the same period than wind, and simulated ground temperature complete the set of inputs.

Two reliable extreme scenarios have been created for the ground temperature. It has been found that friction velocity, turbulent diffusivity coefficients, and turbulent viscous dissipation rate vary less than 5% regarding to the shown-reference values, while Monin-Obukhov length, and surface heat flux vary around 20%. In all cases, the order of magnitude of these magnitudes remains unchanged.

An interval of 0.1 to 10 cm for the surface roughness has been taken on the basis of the values found in the bibliography. We have calculated values of the Monin-Obukhov length in the range of 0 to 100 m as well as a typical hyperbolic behaviour. On Earth, the magnitude of  $L$  matches the one found on Mars. Thus, the height of the surface layer is expected to be similar on both planets.

Friction velocity values have been found to be of the order of  $0.1 \text{ m s}^{-1}$  as on Earth. Such velocity grows with  $z_0$ , since more horizontal momentum is lost to the ground if the surface becomes more roughness. The value of this parameter is very important when considering saltation of grains.

Temperature scale and surface dynamic heat flux show remarkable differences between Mars and Earth. Temperature fluctuations of about 8 K were measured by the PF lander in the turbulent time scale, that is, in seconds or few minutes. Accordingly, we have found maximum values of  $T_*$  around 5 K. Typical eddy temperature fluctuations on Earth are of the order of 0.1 K. On the other hand, maximum values around  $10 \text{ W m}^{-2}$  for  $z_0=1\text{cm}$  for

the surface heat flux have been obtained, while on terrestrial deserts peaks of the order of  $400\text{-}500 \text{ W m}^{-2}$  can be found. Both parameters,  $T_*$  and  $H_0$ , show different values on both planets due to some unique Martian characteristics (by unique we mean that are not met on Earth). As the net radiation that reaches the Martian soil is almost the same than on Earth, and sensible and latent fluxes are much lower on Mars (low atmospheric density and virtual absence of water vapour), the heat conduction in the soil becomes very important [thermal effect of the radiation at the surface has been studied in [30] and [26]. In addition, the thermal inertia is low. This all results in large ground temperature fluctuations (around 80 K through one Sol). Since the air atmospheric density is very low, Martian first few meters air can not be heated so efficiently and does not follow the ground temperature diurnal evolution. Consequently, large temperature gradients are created and therefore higher values of  $T_*$  are observed.

Concerning the turbulent viscous dissipation rate, values between  $10^{-4}\text{-}10^{-1} \text{ m}^2 \text{ s}^{-3}$  have been determined, which is in accordance with the range found in the terrestrial surface layer. This parameter has been obtained supposing that shear and dissipation are almost in balance the whole day. This means that only these two terms become important under stability, while under instability, buoyancy and transport, which are also relevant in magnitude, tend to balance each other. This statement can not be assured for MSL until specific experiments be conducted.

The eddy-transfer coefficients both for momentum and for heat have been found to be  $\sim 0.1 \text{ m}^2 \text{ s}^{-1}$  at 1.3 m during daytime. Both parameters present maximum values corresponding to maximum shear. Values around  $1\text{-}10^1 \text{ m}^2 \text{ s}^{-1}$  are typical for the Earth. Noticing that on Mars, both molecular kinematic viscosity and thermal diffusivity are around  $10^{-3} \text{ m}^2 \text{ s}^{-1}$ , only two orders of magnitude separate molecular diffusion from turbulent diffusion on Mars, while on Earth, turbulent diffusion is five or six orders of magnitude more efficient than molecular exchanges.

The need to include a molecular sublayer into the similarity theory has been explained. Martian density has a low atmospheric value and along with the bluff roughness elements which form the Martian soil cause the difference between  $z_0$  and  $z_{0T}$  to be

come greater. We have used the parameterization proposed by [3] and found that only temperature scale and surface dynamic heat flux are affected by its inclusion. This result was expected since only molecular transfer is important for heat in this sublayer, while for momentum, in addition to molecular transport, pressure fluctuations are very relevant. The main consequences of the inclusion of the molecular sublayer are the decrease of heat flux values (although not drastically) for a given difference between air temperature and ground temperature, and the reduction of the  $z_0$  dependence.

Uncertainties related to the use of Monin-Obukhov similarity have been described. The validity of the universal functions for heat and momentum, and (12) should be tested on MSL. However, until wind (horizontal and vertical component) and temperature be monitored simultaneously at several heights and with high enough sampling rate ( $>1$  Hz), the use of Monin-Obukhov similarity becomes essential in the research of the MSL.

## 6 Acknowledgments

We both thank the firm Arquimea Ingeniería S.L., and the MEC's projects ESP2007-30487-E "El Ciclo de la humedad en la superficie de Marte", and CGL2005-06966-C07-04 for their financial support. We also thank Prof. Sävijärvi (University of Helsinki) for his advice in the use of his model, Prof. Murphy (New Mexico University) for providing us wind data and helping us in the preparation of this paper, and the referees for their useful advises to improve the paper. Prof. Luis Vázquez thanks the partial support from the Dirección General de Investigación of Spain, under grant MTM2005-05573.

## References

- [1] J. C. André, G. De Moor, P. Lacarréré, G. Therry, and R. du Vachar. Modeling the 24-hour evolution of the mean and turbulent structure of the planetary boundary layer. *J. Atmos. Sci.*, 35:1861–1883, 1978.
- [2] P.S. Arya. *Introduction to Micrometeorology*. Academic Press, 2001.
- [3] HW Brutsaert. Exchange processes at the earth-atmosphere interface. *Engineering Meteorology (Plate E, ed.)*. Elsevier: New York, pages 319–369, 1982.
- [4] PR Christensen, JL Bandfield, VE Hamilton, SW Ruff, GL Mehall, N. Gorelick, K. Bender, K. Murray, HH Kieffer, and TN Titus. Mars Global Surveyor Thermal Emission Spectrometer experiment- Investigation description and surface science results. *Journal of Geophysical Research*, 106(E10):23823–23872, 2001.
- [5] MP Golombek, RA Cook, T. Economou, WM Folkner, AFC Haldemann, PH Kallemeyn, JM Knudsen, RM Manning, HJ Moore, TJ Parker, et al. Overview of the Mars Pathfinder Mission and Assessment of Landing Site Predictions. *Science*, 278(5344):1743–1748, 1997.
- [6] R.M. Haberle, H.C. Houben, R. Hertenstein, and T. Herdtle. A Boundary-Layer Model for Mars: Comparison with Viking Lander and Entry Data. *Journal of the Atmospheric Sciences*, 50(11):1544–1559, 1993.
- [7] D.L. Hartmann. *Global Physical Climatology*. 1994.
- [8] SL Hess, RM Henry, CB Leovy, JE Tillman, and JA Ryan. Meteorological results from the surface of Mars-Viking 1 and 2. *Journal of Geophysical Research*, 82:4559–4574, 1977.
- [9] P. Hignett. Roughness lengths for temperature and momentum over heterogeneous terrain. *Boundary-Layer Meteorology*, 68(3):225–236, 1994.
- [10] U. Högström. Non-dimensional wind and temperature profiles in the atmospheric surface layer: A re-evaluation. *Boundary-Layer Meteorology*, 42(1):55–78, 1988.
- [11] J.R. Johnson, W.M. Grundy, and M.T. Lemmon. Dust deposition at the Mars Pathfinder landing site: observations and modeling of visible/near-infrared spectra. *Icarus*, 163(2):330–346, 2003.
- [12] SE Larsen, HE Jørgensen, L. Landberg, and JE Tillman. Aspects Of The Atmospheric Surface Layers On Mars And Earth. *Boundary-Layer Meteorology*, 105(3):451–470, 2002.
- [13] H. Lettau. Note on Aerodynamic Roughness-Parameter Estimation on the Basis of Roughness-Element Description. *Journal of Applied Meteorology*, 8(5):828–832, 1969.
- [14] A. Määttänen and H. Savijärvi. Sensitivity Tests with a One-Dimensional Boundary-Layer Mars Model. *Boundary-Layer Meteorology*, 113(3):305–320, 2004.
- [15] A. S. Monin and A. M. Obukhov. Osnovnye zakonomernosti turbulentnogo peremeshivaniya v prizemnon sloe atmosfery (Basic Laws of Turbulent Mixing in the Atmosphere Near the Ground. *Trudy geofiz. inst. AN SSSR*, 24:163–187, 1954.
- [16] N.E. Putzig, M.T. Mellon, K.A. Kretke, and R.E. Arvidson. Global thermal inertia and surface properties of Mars from the MGS mapping mission. *Icarus*, 173(2):325–341, 2005.
- [17] H. Savijärvi. A model study of the PBL structure on Mars and the earth. *Beitraege zur Physik der Atmosphaere*, 64:219–229, 1991.
- [18] H. Savijärvi. A model study of the atmospheric boundary layer in the Mars Pathfinder lander conditions. *Quarterly Journal of the Royal Meteorological Society*, 125(554):483–493, 1999.
- [19] H. Savijärvi, A. Määttänen, J. Kauhanen, and A.M. Harri. Mars Pathfinder: New data and new model simulations. *Quarterly Journal of the Royal Meteorological Society*, 130(597):669–683, 2004.

- [20] H. Savijärvi and T. Siili. The Martian Slope Winds and the Nocturnal PBL Jet. *Journal of the Atmospheric Sciences*, 50(1):77–88, 1993.
- [21] JT Schofield, JR Barnes, D. Crisp, RM Haberle, S. Larsen, JA Magalhaes, JR Murphy, A. Seiff, and G. Wilson. The Mars Pathfinder Atmospheric Structure Investigation/Meteorology (ASI/MET) Experiment. *Science*, 278(5344):1752, 1997.
- [22] Science. Mars Pathfinder-Images. *Science*., 278:1734–1742, 1997.
- [23] R.B. Stull. *An Introduction to Boundary Layer Meteorology*. Springer, 1988.
- [24] J.L. Sutton, C.B. Leovy, and J.E. Tillman. Diurnal Variations of the Martian Surface Layer Meteorological Parameters During the First 45 Sols at Two Viking Lander Sites. *Journal of the Atmospheric Sciences*, 35(12):2346–2355, 1978.
- [25] J.E. Tillman, L. Landberg, and S.E. Larsen. The Boundary Layer of Mars: Fluxes, Stability, Turbulent Spectra, and Growth of the Mixed Layer. *Journal of the Atmospheric Sciences*, 51(12):1709–1727, 1994.
- [26] L. Vázquez, M.P. Zorzano, and S. Jimenez. Spectral information retrieval from integrated broadband photodiode Martian ultraviolet measurements. *Optics Letters*, 32(17):2596–2598, 2007.
- [27] JC Wyngaard and OR Coté. The Budgets of Turbulent Kinetic Energy and Temperature Variance in the Atmospheric Surface Layer. *Journal of the Atmospheric Sciences*, 28(2):190–201, 1971.
- [28] X. Zeng and R.E. Dickinson. Effect of Surface Sublayer on Surface Skin Temperature and Fluxes. *Journal of Climate*, 11(4):537–550, 1998.
- [29] S.S. Zilitinkevich. *Dynamics of the Atmospheric Boundary Layer*. Leningrad Gidrometeor, 1970.
- [30] M.P. Zorzano and L. Vázquez. Remote temperature retrieval from heating or cooling targets. *Optics Letters*, 31(10):1420–1422, 2006.